Supporting Information

Detailed Compositional Characterization of the 2014 Bangladesh Furnace Oil Released into the World's Largest Mangrove Forest

Huan Chen[†], Robert, K. Nelson[‡], Robert F. Swarthout[§], Gary Shigenaka[⊥], André H.B. de Oliveira[¶], Christopher M. Reddy[‡], and Amy M. McKenna[†,*]

[†] National High Magnetic Field Laboratory, Florida State University, 1800 East Paul Dirac Dr., Tallahassee, FL 32310, United States

[‡]Department of Marine Chemistry and Geochemistry, Woods Hole Oceanographic Institution, Woods Hole, MA 02543, United States

[§]Department of Chemistry and Environmental Science Program, Appalachian State University, Boone, NC 28608, United States

[⊥]Emergency Response Division, National Oceanic and Atmospheric Administration, 7600 Sand Point Way, NE, Seattle, WA 98115, United States

[¶] Laboratory for Assessment of Organic Contaminants (LACOr), Institute of Marine Sciences-Federal University of Ceará (LABOMAR-UFC), Av. Abolição, 3207-Meireles, CEP: 60165-081 Fortaleza, CE, Brazil.

- Corresponding author: Amy M. McKenna

Number of pages: 17

Number of figures: 9

Number of tables: 1

Materials and Methods

Elemental analysis:

Elemental analysis was performed for both Bangladesh furnace oil and Texas City IFO with a Thermo Finnigan Elemental Analyzer (FLASH EA 112, San Jose, CA, USA) to determine CHNS (run 1) and O content (run 2) in two separate experiments for both Bangladesh and Texas. For CHNS analysis, 1.5-2.75 mg of sample was placed in a tin cup, crushed to form a sphere, and placed in the autosampler. All samples were analyzed in quadruplicate. Calibration of the instrument is provided by the analysis of standards of known elemental content, and all quadruplicate runs included a separate, independent standard not used in the initial calibration. A similar procedure was followed for oxygen measurements, but with a silver cup. Lubricant reference material 0104 (Thermo) was used as the standard to calibrate the instrument and Lubricant oil 100608 (Microlab s.n.c.) was analyzed together with samples as an independent standard in each run. For O analysis, about 1 mg samples were placed in silver cups and measured by pyrolysis at 1060 °C. Standard materials 2, 5-bis-(5-tert-butyl-benzoxazol-2-yl)-thiophene (BBOT) was used for calibration, and the measurements were within ±0.4% of theoretical values.

GC×GC-FID and GC×GC-TOF MS analysis

We used GC × GC-FID methods described in detail previously.[1] Briefly, 1 µL of Bangladesh furnace oil and Texas City IFO dissolved in n-hexane (50 mg/mL) was injected in a GC×GC-FID system with a dual stage cryogenic modulator (Leco, Saint Joseph, MI), equipped with a Restek Rtx-1 first dimension column (60 m, 0.25 mm I.D., 0.25 µm film thickness) and a SGE BPX50 second dimension column (1.5 m, 0.10 mm I.D., 0.10 µm film thickness). The inlet temperature was held at 300 °C. The injection mode was splitless, and the carrier gas was hydrogen at a constant flow rate of 1.00 mL/min. The first oven was programmed isothermal at 40 °C for 10 min, 40 to 340 °C at 1.25 °C/min (held for 5 min). The second oven was programmed as follows: isothermal at 45 °C for 10 min, 45 to 355 °C at 1.29 °C/min (held for 5 min). The modulation period was 15 s. PAHs compounds were identified based on established elution order[2] and in comparison with pure PAHs standards.

A GC×GC-time of flight mass spectrometer (GC×GC-TOF) system equipped with a dual stage cryogenic modulator (Leco, Saint Joseph, Michigan) was used to acquire mass spectra of the analytes. Both samples were injected in splitless mode, and the purge vent was opened at 1 minute. The inlet temperature was 300 °C. The first-dimension column was a nonpolar Restek Rtx-1MS, (60m length, 0.25 mm I.D., 0.25 µm film thickness) and second-dimension separations were performed on a 50% phenyl polysilphenylene-siloxane column (SGE BPX50, 1.25 m length, 0.10 mm I.D., 0.1 µm film thickness). The first dimension column oven was programmed to remain isothermal

at 70 °C for 0.2 min and ramped from 70 to 330 °C at 2 °C/min. Then the oven remained isothermal at 330 °C for 0.5 min. The second dimension oven was programmed to remain isothermal at 75 °C for 0.2 min and then ramped from 75 to 335 °C at 2 °C/min. The oven remained isothermal at 335°C for 0.5 min. The modulation period was 10 s. The carrier gas was helium at a constant flow rate of 1 mL/min. The TOF MS detector signal was sampled at a data rate of 50 Hz. Chromatographic peaks were identified with pure standards or tentatively identified based on retention times in both dimensions and mass spectral matches (above 80% similarity; NIST/EPA/NIH 05 Mass Spectral Library).

FT-ICR MS analysis

Ionization: APPI Source: An atmospheric pressure photoionization (APPI) source (Thermo-Fisher Scientific, San Jose, CA) was coupled to the first stage of a custom-built FT-ICR mass spectrometer through a custom-built interface.[3] To minimize ion fragmentation the tube lens was set to 50 V and the heated metal capillary current to 4.5 A. A Hamilton gastight syringe (2.5 mL) and syringe pump were used to deliver samples (50 µL/min) to the heated vaporizer region (300 °C) of the APPI source, where N_2 sheath gas (50 psi) facilitates nebulization, while the auxiliary port remained plugged. After nebulization, gas-phase neutral analyte molecules exit the heated vaporizer region as a confined jet. Photoionization is initiated by a krypton vacuum ultraviolet gas discharge lamp (Syagen Technology, Inc, Tustin, CA) that produces 10-10.2 eV photons (120 nm). Toluene increases the ionization efficiency for nonpolar aromatic compounds through dopant-assisted APPI[4] through charge exchange[5] and proton transfer[6] reactions between ionized toluene molecules and neutral analyte molecules. Protonated ions exhibit half-integer double bond equivalents values (DBE = c – h/2 + n/2 + 1), calculated from ion elemental composition (C*c*H*h*N*n*O*o*S*s*), and may be distinguished from radical cations with integer DBE values.[7]

Ionization: ESI Source: The oils from the two spills were also analyzed by positive and Negative Electrospray Ionization (ESI). Both samples were dissolved separately into toluene to yield stock solutions at 1 mg/mL concentration. The samples were further diluted to 500 µg/mL with equal parts (vol: vol) of methanol spiked with 4% (by volume) formic acid (positive ESI) or 0.25% (by volume) tetramethylammonium hydroxide (negative ESI) to ensure efficient protonation/ deprotonation. Sample solutions were pumped through a microelectrospray source[8] (50 µm i.d. fused silica emitter) at 0.5 µL/min by a syringe pump. Conditions for negative ion formation were emitter voltage, -2.5 kV; tube lens, -250V and heated metal capillary current, 5.0 A. Positive ion formation occurred at the same conditions as for negative ions, but with positive values.

9.4 T FT-ICR Mass Spectrometer: The two oil samples were analyzed with a custom-built FT-ICR mass spectrometer[9] equipped with a 9.4 Tesla horizontal 220 mm bore diameter superconducting solenoid magnet operated at room temperature, and a modular ICR data station (Predator)[10] facilitated instrument control, data acquisition, and data analysis. Positive ions generated at atmospheric pressure were accumulated in an external quadrupole (130 ms), passed through an rf-only quadrupole into an

octopole equipped with tilted wire extraction electrodes for improved ion extraction and transmission.[11] Helium gas introduced into the octopole collisionally cools ions prior to transfer through rf-only quadrupoles (total length 127 cm) equipped with an auxiliary rf waveform[12] into a 7-segment open cylindrical cell[13] with capacitively coupled excitation electrodes based on the Tolmachev configuration.[14] 100 individual transients of 6.8s duration were signal averaged, apodized with a half-Hanning weight function, and zero-filled once prior to fast Fourier transformation. Data was collected at maximum memory depth of the data station hardware (16 million samples), apodized with a single sided Hanning apodization, zero-filled to 16 megasample (16777216 samples or 224). An additional zero fill brings the pre FT data packet to 32 megasample. Due to increased complexity at higher m/z, broadband phase correction[15] was applied to the mass spectrum to increase the resolution of isobaric species as previously described.[16]

For all mass spectra, the achieved mass spectral resolving power approached the theoretical limit[17] across the entire mass range, e.g., average resolving power, m/Δm50%, in which Δm50% is mass spectral peak width at half maximum peak height was ~1,000,000 – 1,500,000 at m/z 500.

Mass Calibration and Data Analysis: ICR frequencies were converted to ion masses based on the quadrupolar trapping potential approximation.[18, 19] Each m/z spectrum was internally calibrated with respect to an abundant homologous alkylation series whose members differ in mass by an additional methylene unit (14.01565 Da), and confirmed by isotopic fine structure based on the "walking" calibration equation.[20] Experimentally measured masses were converted from the International Union of Pure and Applied Chemistry (IUPAC) mass scale to the Kendrick mass scale[21] for rapid identification of homologous series for each heteroatom class (i.e., species with the same C*c*H*h*N*n*O*o*S*s* content, differing only by degree of alkylation). For each elemental composition, C*c*H*h*N*n*O*o*S*si*, the heteroatom class, type (double bond equivalents, DBE = number of rings plus double bonds to carbon, (DBE = C - h/2 + n/2 + 1)[22] and carbon number, c, were tabulated for data visualization.

1. Aeppli, C.; Nelson, R. K.; Radović, J. R.; Carmichael, C. A.; Valentine, D. L.; Reddy, C. M., Recalcitrance and degradation of petroleum biomarkers upon abiotic and biotic natural weathering of Deepwater Horizon oil. *Environmental Science & Technology* **2014,** 48, (12), 6726-6734.
2. Skoczyńska, E.; Korytár, P.; Boer, J. d., Maximizing chromatographic information from environmental extracts by GCxGC-ToF-MS. *Environmental Science and Technology* **2008,** 42, (17), 6611-6618.
3. Purcell, J. M.; Hendrickson, C. L.; Rodgers, R. P.; Marshall, A. G., Atmospheric Pressure Photoionization Fourier Transform Ion Cyclotron Resonance Mass Spectrometry for Complex Mixture Analysis. *Anal. Chem.* **2006,** 78, (16), 5906-5912.
4. Robb, D. B.; Blades, M. W., Factors affecting primary ionization in dopant-assisted atmospheric pressure photoionization (DA-APPI) for LC/MS. *J. Am. Soc. Mass Spectrom.* **2006,** 17, (2), 130-138.

5. Smith, D. F.; Robb, D. B.; Blades, M. W., Comparison of Dopants for Charge Exchange Ionization of Nonpolar Polycyclic Aromatic Hydrocarbons with Reversed-Phase LC-APPI-MS. *J. Am. Soc. Mass Spectrom.* **2009,** 20, (1), 73-79.
6. Purcell, J. M.; Rodgers, R. P.; Hendrickson, C. L.; Marshall, A. G., Atmospheric Pressure Photoionization Proton Transfer for Complex Organic Mixtures Investigated by Fourier Transform Ion Cyclotron Resonance Mass Spectrometry. *J. Am. Soc. Mass Spectrom.* **2007,** 18, 1682-1689.
7. McKenna, A. M.; Purcell, J. M.; Rodgers, R. P.; Marshall, A. G., Identification of vanadyl porphyrins in a heavy crude oil and raw asphaltene by atmospheric pressure photoionization Fourier transform ion cyclotron resonance (FT-ICR) mass spectrometry. *Energy Fuels* **2009,** 23, (4), 2122-2128.
8. Emmett, M. R.; White, F. M.; Hendrickson, C. L.; Shi, S. D. H.; Marshall, A. G., Application of micro-electrospray liquid chromatography techniques to FT-ICR MS to enable high-sensitivity biological analysis. *Journal of the American Society for Mass Spectrometry* **1998,** 9, (4), 333-340.
9. Kaiser, N. K.; Quinn, J. P.; Blakney, G. T.; Hendrickson, C. L.; Marshall, A. G., A Novel 9.4 Tesla FTICR Mass Spectrometer with Improved Sensitivity, Mass Resolution, and Mass Range. *J. Am. Soc. Mass Spectrom.* **2011,** 22, (8), 1343-1351.
10. Blakney, G. T.; Hendrickson, C. L.; Marshall, A. G., Predator data station: A fast data acquisition system for advanced FT-ICR MS experiments. *Int. J. Mass Spectrom.* **2011,** 306, (2-3), 246-252.
11. Wilcox, B. E.; Hendrickson, C. L.; Marshall, A. G., Improved ion extraction from a linear octopole ion trap: SIMION analysis and experimental demonstration. *J. Am. Soc. Mass Spectrom.* **2002,** 13, 1304-1312.
12. Kaiser, N. K.; Savory, J. J.; Hendrickson, C. L., Controlled ion ejection from an external trap for extended *m/z* range in FT-ICR mass spectrometry. *J. Am. Soc. Mass Spectrom.* **2014,** 25, 943-949.
13. Kaiser, N. K.; Savory, J. J.; McKenna, A. M.; Quinn, J. P.; Hendrickson, C. L.; Marshall, A. G., Electrically compensated Fourier transform ion cyclotron resonance cell for complex mixture mass analysis. *Anal. Chem.* **2011,** 83, (17), 6907-6910.
14. Tolmachev, A. V.; Robinson, E. W.; Wu, S.; Smith, R. D.; Pasa-Tolic, L., Trapping radial electric field optimization in compensated FTICR cells. *J Am Soc Mass Spectrom* **2011,** 22, (8), 1334-1342.
15. Beu, S. C.; Blakney, G. T.; Quinn, J. P.; Hendrickson, C. L.; Marshall, A. G., Broadband phase correction of FT-ICR mass spectra via simultaneous excitation and detection. *Anal. Chem.* **2004,** 76, (19), 5756-5761.
16. Xian, F.; Hendrickson, C. L.; Blakney, G. T.; Beu, S. C.; Marshall, A. G., Automated Broadband Phase Correction of Fourier Transform Ion Cyclotron Resonance Mass Spectra. *Anal. Chem.* **2010,** 82, (21), 8807-8812.
17. Marshall, A. G.; Hendrickson, C. L.; Jackson, G. S., Fourier transform ion cyclotron mass spectrometry: A primer. *Mass Spectrom. Rev.* **1998,** 17, (1), 1-35.
18. Shi, S. D. H.; Drader, J. J.; Freitas, M. A.; Hendrickson, C. L.; Marshall, A. G., Comparison and interconversion of the two most common frequency-to-mass calibration functions for Fourier transform ion cyclotron resonance mass spectrometry. *International Journal of Mass Spectrometry* **2000,** 195, 591-598.
19. Grosshans, P. B.; Shields, P. J.; Marshall, A. G., Comprehensive Theory of the Fourier-Transform Ion-Cyclotron Resonance Signal for All Ion Trap Geometries. *Journal of Chemical Physics* **1991,** 94, (8), 5341-5352.
20. Savory, J. J.; Kaiser, N. K.; McKenna, A. M.; Xian, F.; Blakney, G. T.; Rodgers, R. P.; Hendrickson, C. L.; Marshall, A. G., Parts-Per-Billion Fourier Transform Ion Cyclotron

Resonance Mass Measurement Accuracy with a "Walking" Calibration Equation. *Anal. Chem.* **2011,** 83, (5), 1732-1736.
21. Kendrick, E., A Mass Scale Based on CH_2 = 14.0000 for High Resolution Mass Spectrometry of Organic Compounds. *Anal. Chem.* **1963,** 35, (13), 2146-2154.
22. McLafferty, F. W.; Turecek, F., *Interpretation of Mass Spectra*. 4th ed. ed.; University Science Books: Mill Valley, CA, 1993; p 371.

Supporting Information Figures

Figure S1. Local children cleaning oil spill, Sundarbans, Bangladesh. Photo Credit: Kallol Mustafa.

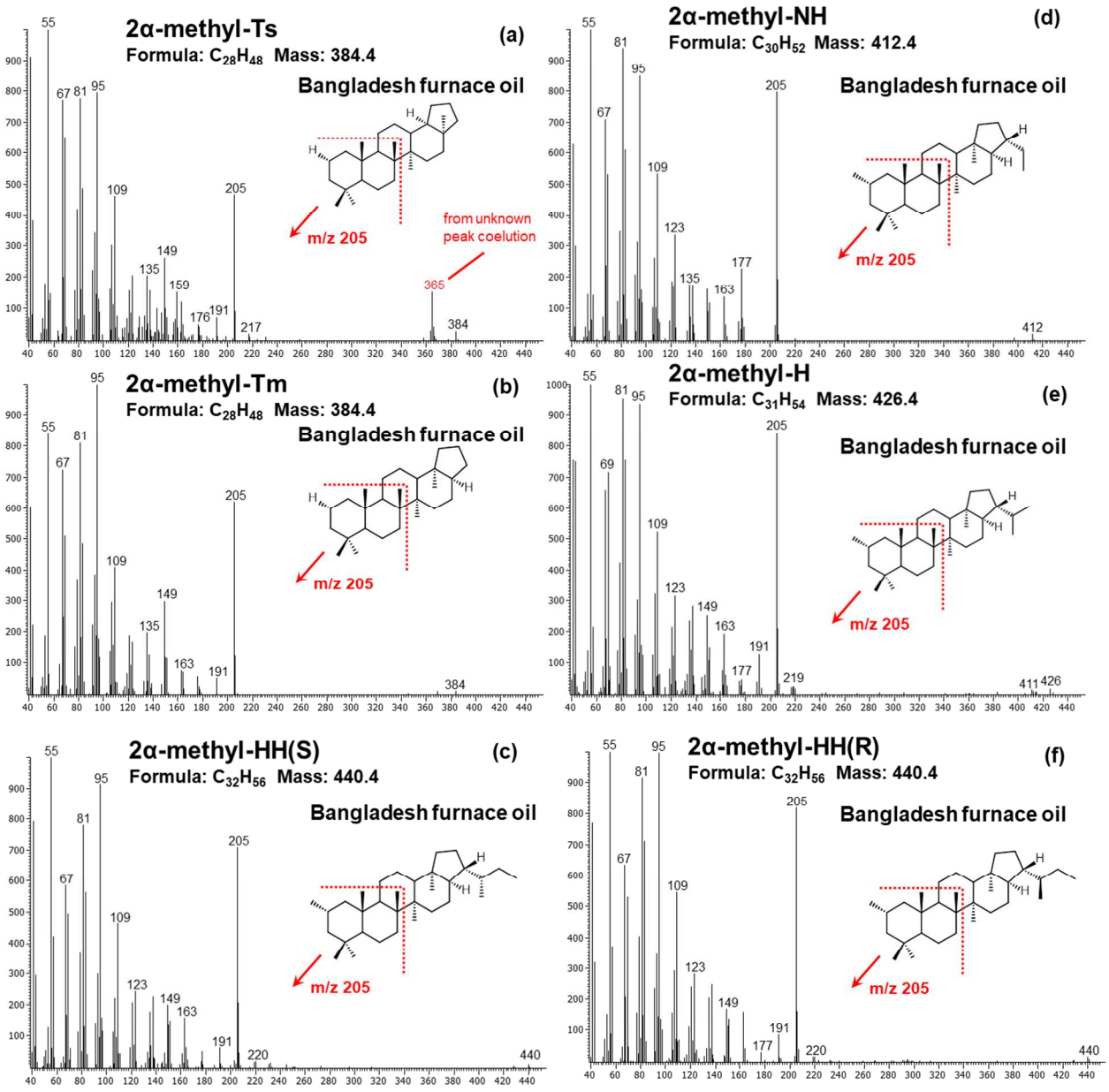

Figure S2. GC×GC-TOF mass spectra for each biomarker compound from Bangladesh furnace oil.

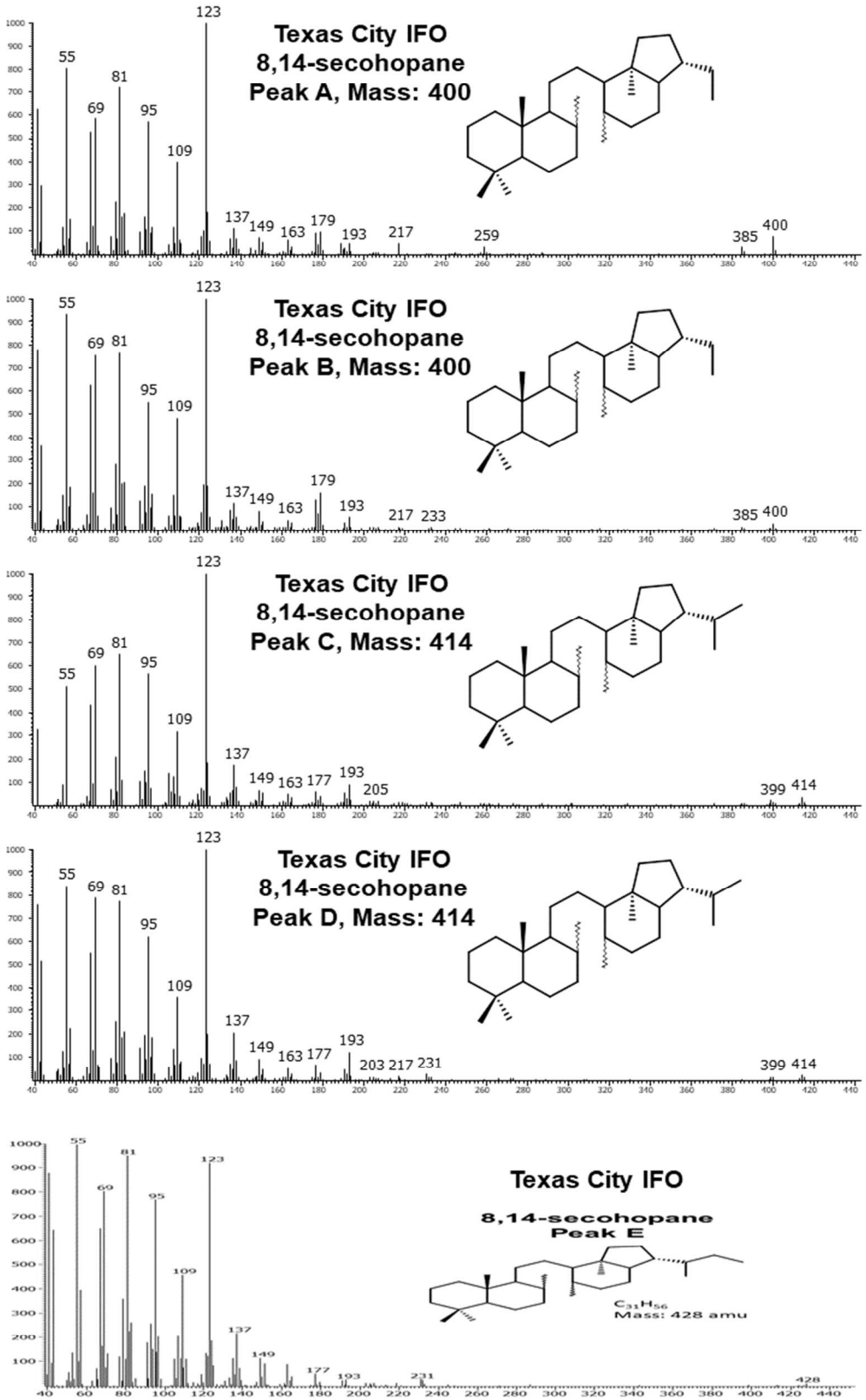

Figure S3. GC×GC-TOF mass spectra for each biomarker compound from Texas IFO.

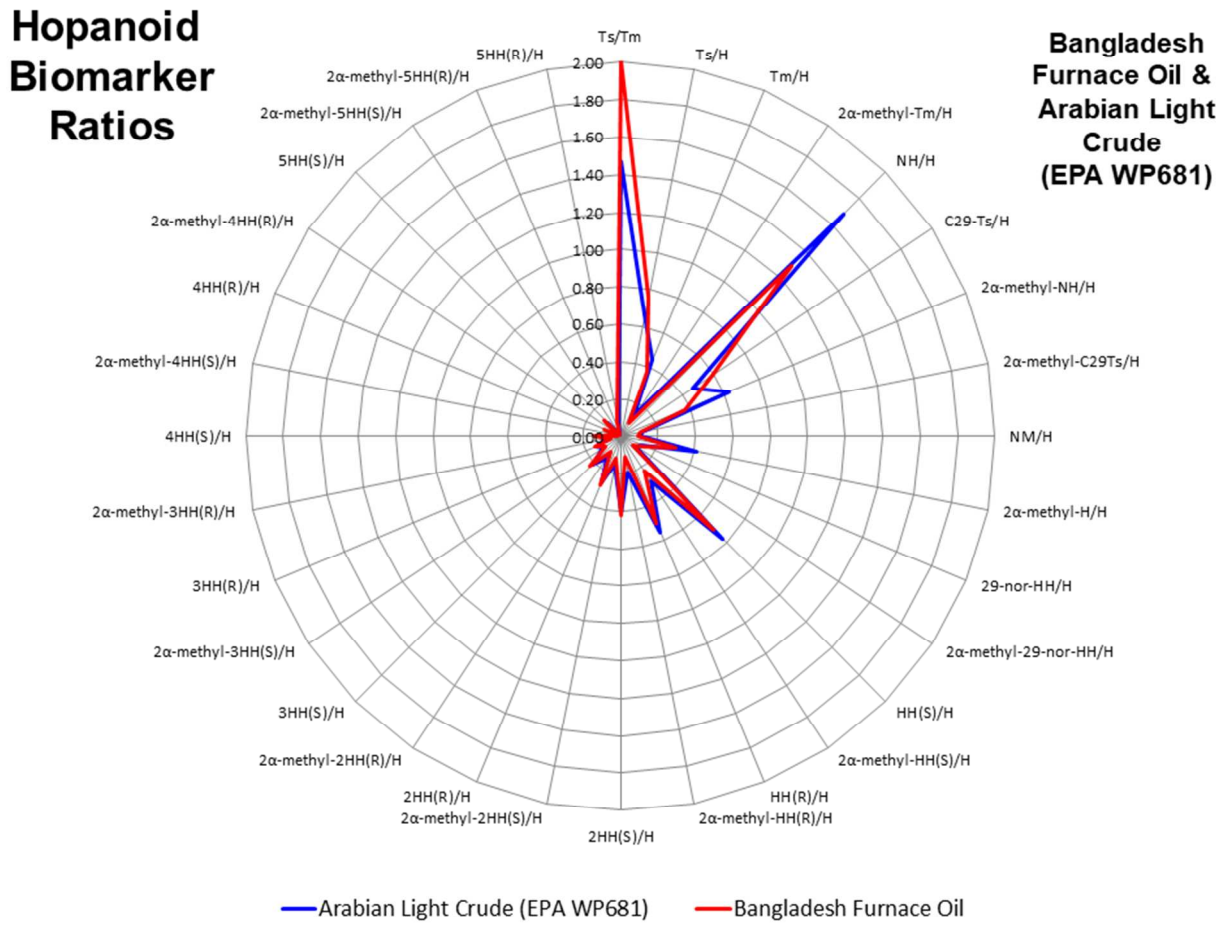

Figure S4. Spider diagrams for the Bangladesh furnace oil and Arabian Light Crude standard (EPA WP681) constructed from thirty diagnostic biomarker ratios Ts/Tm, (5HH(R)/H, 2α-methyl-5HH(R)/H, 2α-methyl-5HH(S)/H, 5HH(S)/H, 2α-methyl-4HH(R)/H, 4HH(R)/H, 2α-methyl-4HH(S)/H, 4HH(S)/H, 2α-methyl-3HH(R)/H, 3HH(R)/H, 2α-methyl-3HH(S)/H, 3HH(S)/H, 2α-methyl-2HH(R)/H, 2HH(R)/H, 2α-methyl-2HH(S)/H, 2HH(S)/H, 2α-methyl-HH(R)/H, HH(R)/H, 2α-methyl-HH(S)/H, HH(S)/H, 2α-methyl-HH(S)/H, HH(S)/H, 2α-methyl-29-nor-HH/H, 29-nor-HH/H, 2α-methyl-H/H, NM/H, 2α-methyl-C29Ts/H, 2α-methyl-NH/H, C29-Ts/H, NH/H, 2α-methyl-Tm/H, Tm/H, and Ts/H. The diagrams for both samples demonstrate the similarity to the Arabian Light Crude standard.

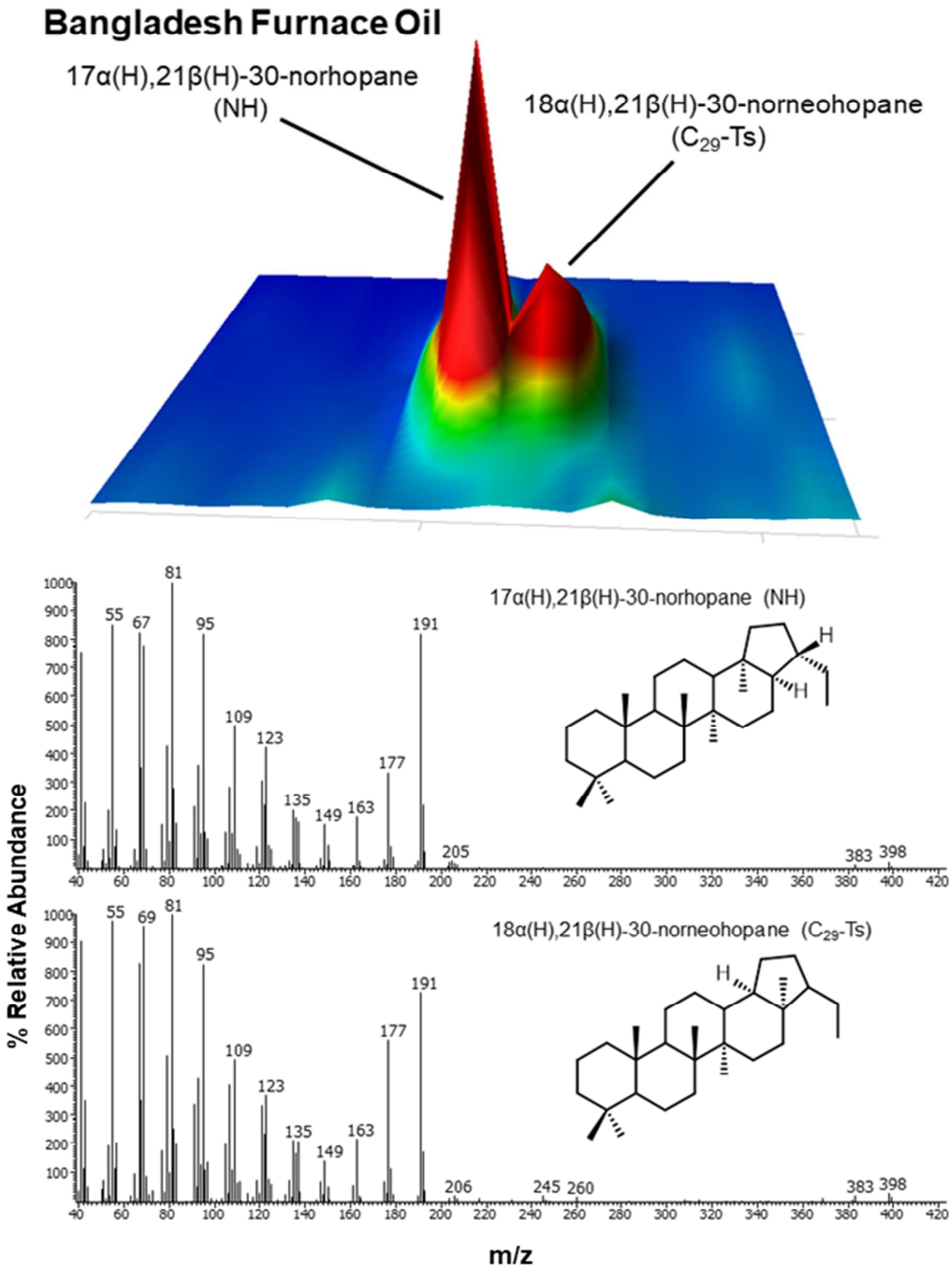

Figure S5. Zoomed-in view of GC×GC-FID chromatogram of Bangladesh furnace oil that highlights the chromatographic resolution between NH and C_{29}-Ts.

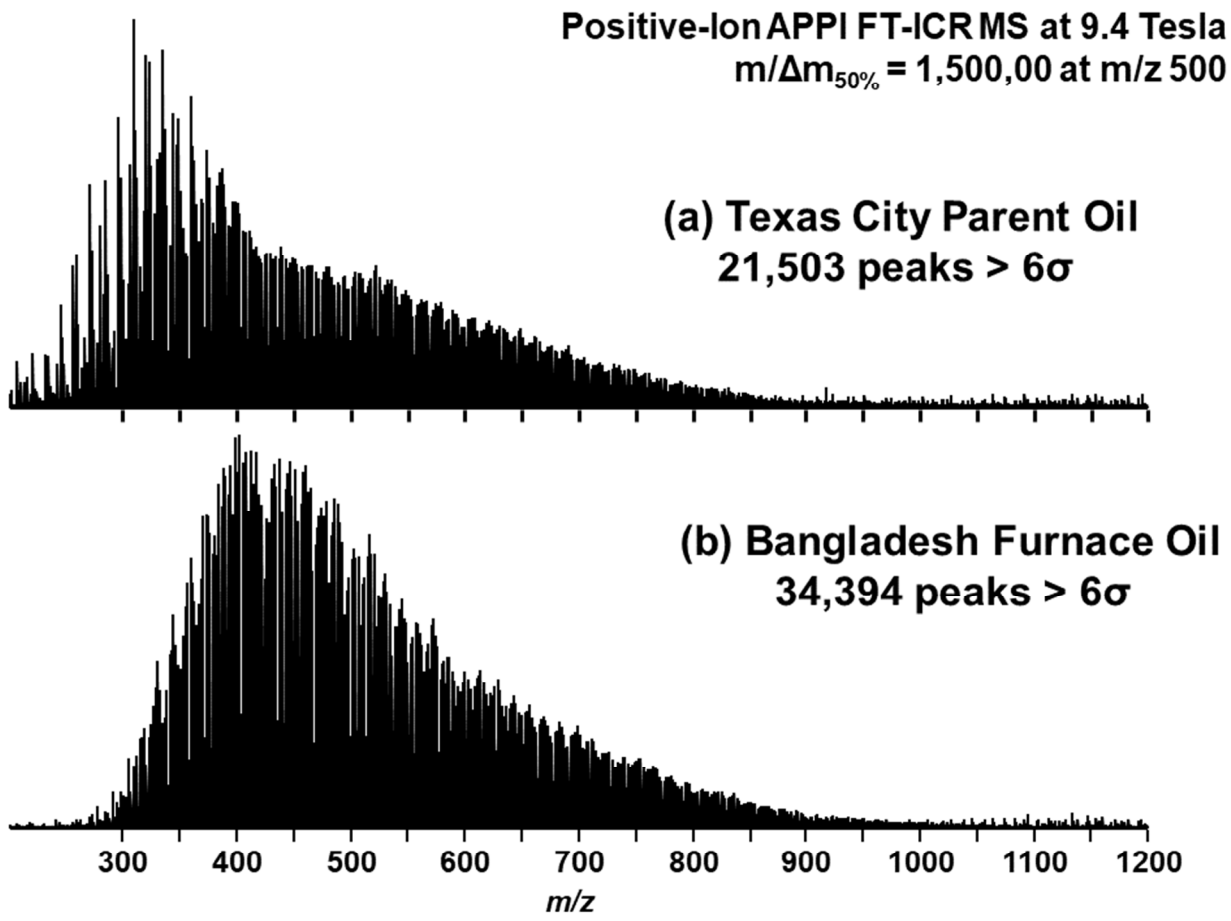

Figure S6. Broadband positive-ion APPI FT-ICR mass spectra at 9.4 tesla for the Texas City IFO (a) and Bangladesh furnace oil (b). The blended IFO distribution highlights a bimodal distribution that corresponds to the low molecular weight cutting oil (250<m/z<450) and higher molecular weight residue (450<m/z<950). Although reported as a blended product, the furnace oil distribution is centered at m/z 425 similar to whole, heavy crudes.

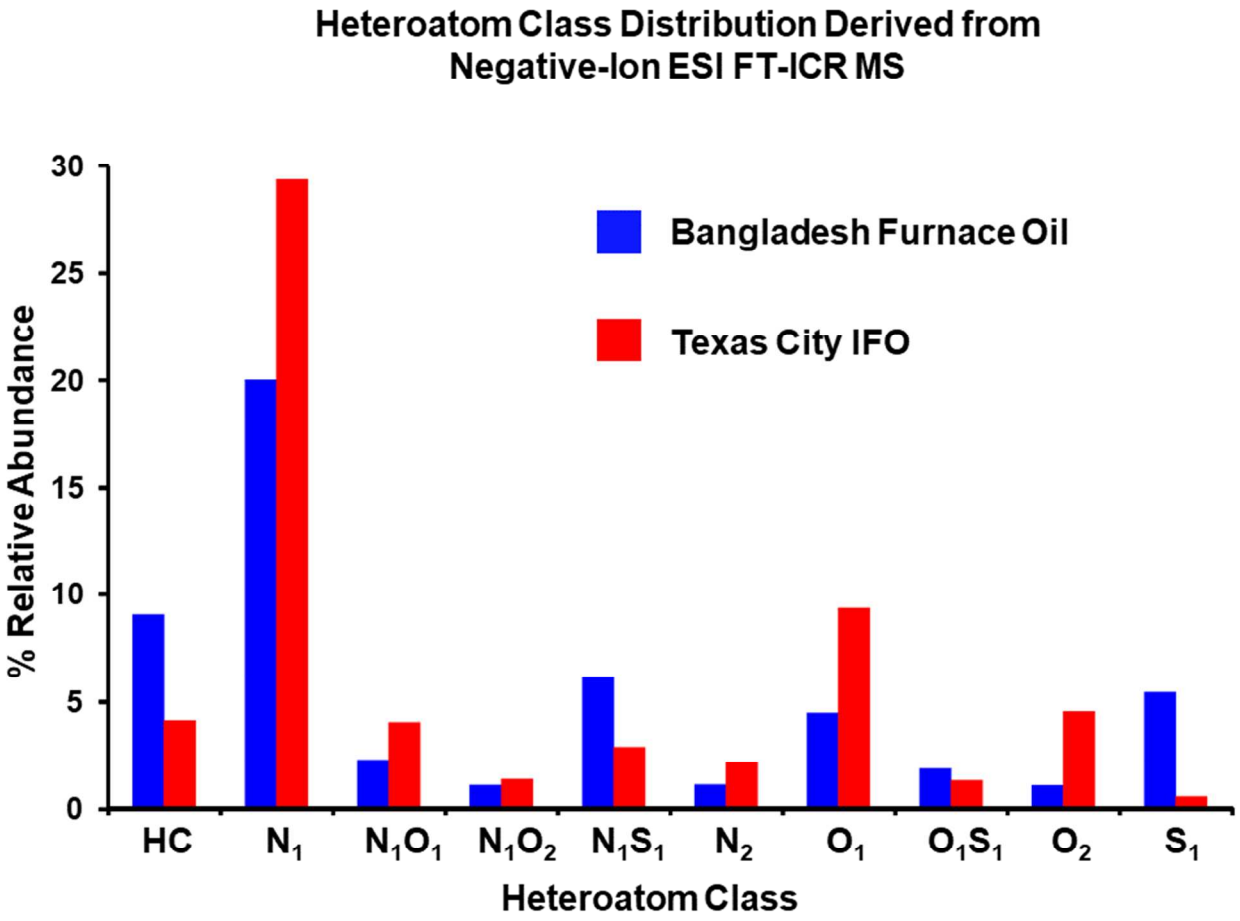

Figure S7. Heteroatom class distribution (heteroatom content) for Bangladesh furnace oil and Texas City IFO derived from negative-ion ESI FT-ICR MS. HC denotes molecules containing only hydrogen and carbon.

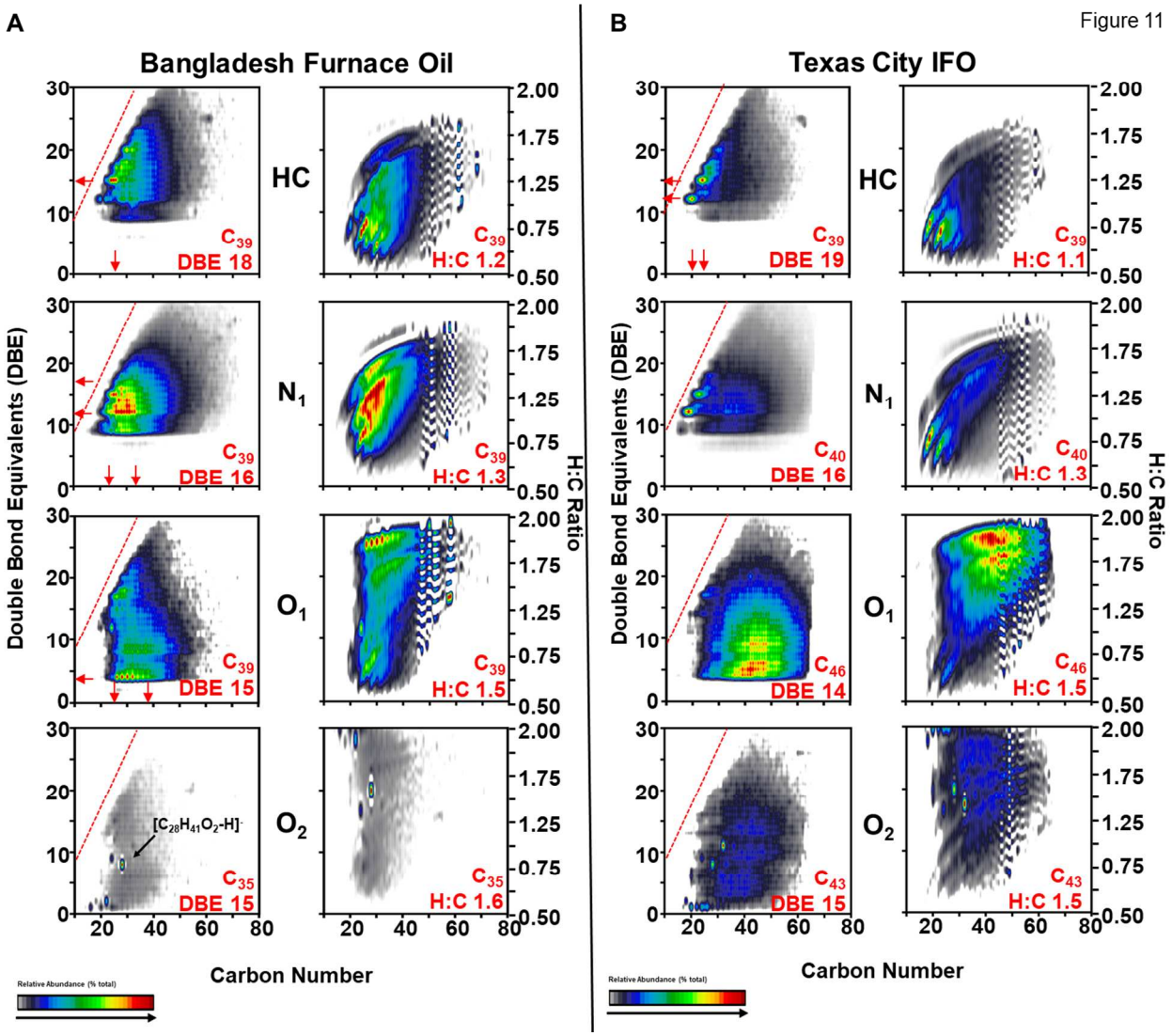

Figure S8. Isoabundance-contoured plots of double bond equivalents (DBE, left) and H:C ratio (right) versus carbon number for acidic hydrocarbons (HC), N1, O1 and O2 classes obtained from negative-ion electrospray ionization with tetramethylammonium hydroxide FT-ICR MS for (a) Bangladesh furnace oil and (b) IFO from Texas City. Relative abundance-weighted averaged DBE, H:C ratio, and carbon numbers calculated from neutral elemental compositions are shown in red for each heteroatom class.

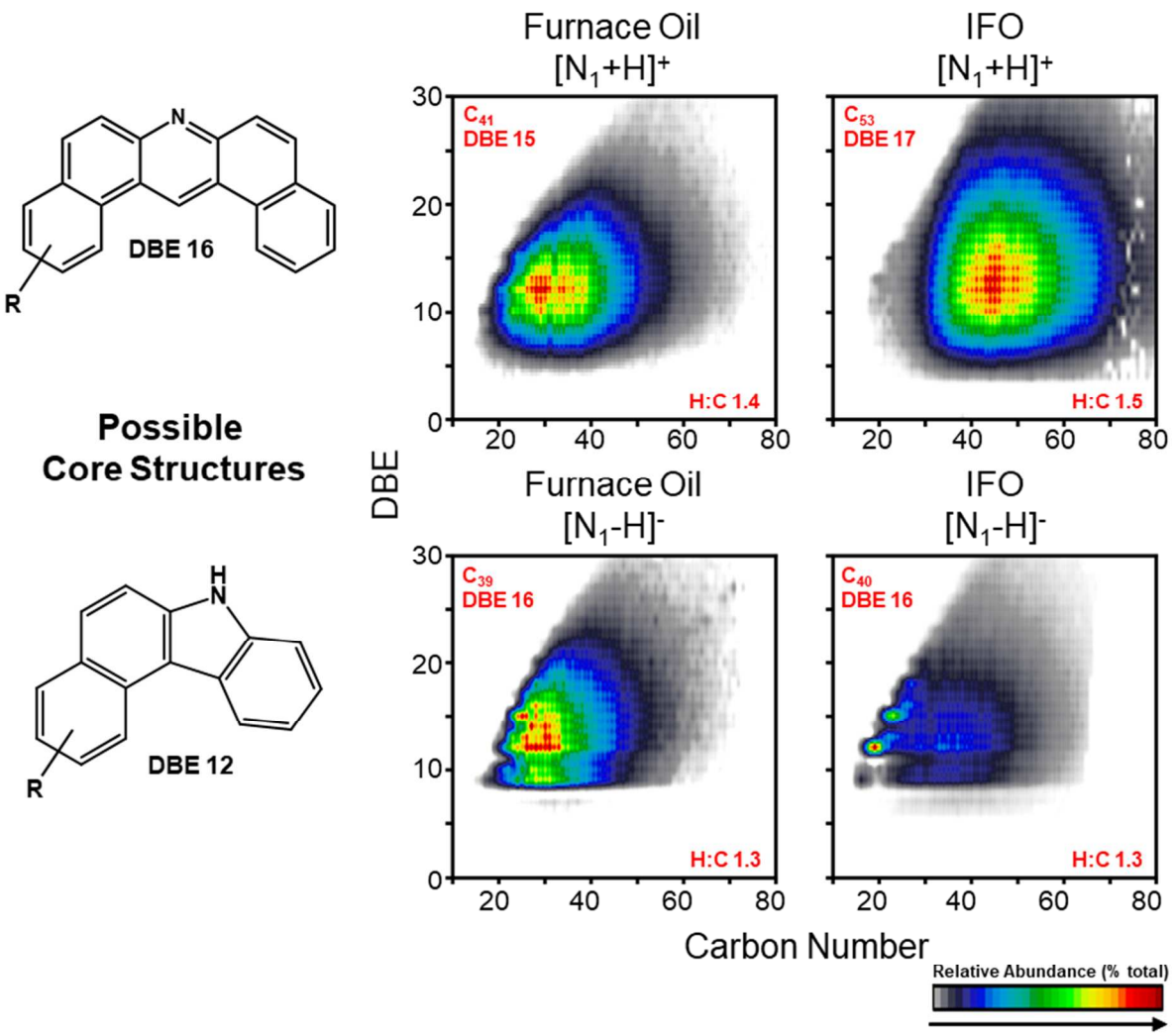

Figure S9. DBE versus carbon number images for the N1 class derived from positive ion electrospray ionization (top) and negative ion electrospray ionization (bottom) for Bangladesh furnace oil and IFO from Texas City. Nitrogen compounds in positive electrospray correspond to six-member ring pyridinnic nitrogen and are protonated, whereas negative ion electrospray selectively ionizes five-member ring pyrrolic nitrogen compounds through deprotonation. Two possible core structures are shown for each nitrogen type.

Table S1. List of biomarkers abbreviations, names, formulas, and atomic mass data.

Compound ID	Hopanes	Mass
Ts	18α(H)-22,29,30-trinorneohopane ($C_{27}H_{46}$)	370
Tm	17α(H)-22,29,30-trinorhopane ($C_{27}H_{46}$)	370
NH	17α(H),21β(H)-30-norhopane ($C_{29}H_{50}$)	398
C_{29}-Ts	18α(H),21β(H)-30-norneohopane ($C_{29}H_{50}$)	398
NM	17β(H),21α(H)-30-norhopane ($C_{29}H_{50}$)	398
H	17α(H),21β(H)-hopane ($C_{30}H_{52}$)	412
29-nor-HH	17α(H),21β(H)-29-norhomohopane ($C_{30}H_{52}$)	412
HH(S)	17α(H),21β(H)-22S-homohopane ($C_{31}H_{54}$)	426
HH(R)	17α(H),21β(H)-22R-homohopane ($C_{31}H_{54}$)	426
2HH(S)	17α(H),21β(H)-22S-bishomohopane ($C_{32}H_{56}$)	440
2HH(R)	17α(H),21β(H)-22R-bishomohopane ($C_{32}H_{56}$)	440
3HH(S)	17α(H),21β(H)-22S-trishomohopane ($C_{33}H_{58}$)	454
3HH(R)	17α(H),21β(H)-22R-trishomohopane ($C_{33}H_{58}$)	454
4HH(S)	17α(H),21β(H)-22S-tetrakishomohopane ($C_{34}H_{60}$)	468
4HH(R)	17α(H),21β(H)-22R-tetrakishomohopane ($C_{34}H_{60}$)	468
5HH(S)	17α(H),21β(H)-22S-pentakishomohopane ($C_{35}H_{62}$)	482
5HH(R)	17α(H),21β(H)-22R-pentakishomohopane ($C_{35}H_{62}$)	482
Compound ID	**2α-Methyl-Hopanes**	**Mass**
2α-methyl-Ts	2α-methyl-18α(H)-22,29,30-trinorneohopane ($C_{28}H_{48}$)	384
2α-methyl-Tm	2α-methyl-17α(H)-22,29,30-trinorhopane ($C_{28}H_{48}$)	384
2α-methyl-NH	2α-methyl-17α(H),21β(H)-30-norhopane ($C_{30}H_{52}$)	412
2α-methyl-C_{29}-Ts	2α-methyl-18α(H),21β(H)-30-norneohopane ($C_{30}H_{52}$)	412
2α-methyl-NM	2α-methyl 17β(H),21α(H)-30-norhopane ($C_{30}H_{52}$)	412
2α-methyl-H	2α-methyl-17α(H),21β(H)-hopane ($C_{31}H_{54}$)	426

2α-methyl-29-nor-HH	2α-methyl-17α(H),21β(H)-29-norhomohopane ($C_{31}H_{54}$)	426
2α-methyl-HH(S)	2α-methyl-17α(H),21β(H)-22S-homohopane ($C_{32}H_{56}$)	440
2α-methyl-HH(R)	2α-methyl-17α(H),21β(H)-22R-homohopane ($C_{32}H_{56}$)	440
2α-methyl-2HH(S)	2α-methyl-17α(H),21β(H)-22S-bishomohopane ($C_{33}H_{58}$)	454
2α-methyl-2HH(R)	2α-methyl-17α(H),21β(H)-22R-bishomohopane ($C_{33}H_{58}$)	454
2α-methyl-3HH(S)	2α-methyl-17α(H),21β(H)-22S-trishomohopane ($C_{34}H_{60}$)	468
2α-methyl-3HH(R)	2α-methyl-17α(H),21β(H)-22R-trishomohopane ($C_{34}H_{60}$)	468
2α-methyl-4HH(S)	2α-methyl-17α(H),21β(H)-22S-tetrakishomohopane ($C_{35}H_{62}$)	482
2α-methyl-4HH(R)	2α-methyl-17α(H),21β(H)-22R-tetrakishomohopane ($C_{35}H_{62}$)	482
2α-methyl-5HH(S)	2α-methyl-17α(H),21β(H)-22S-pentakishomohopane ($C_{36}H_{64}$)	496
2α-methyl-5HH(R)	2α-methyl-17α(H),21β(H)-22R-pentakishomohopane ($C_{36}H_{64}$)	496